Int. J. Electrochem. Sci., 13 **(2018)** 4243 – 4250, doi: 10.20964/2018.05.78

International Journal of ELECTROCHEMICAL SCIENCE
www.electrochemsci.org

Short Communication

Multilayered Electrochromic Films of Metal Hexacyanoferrates Nanoparticles

Hisashi Tanaka[1], *Hiroshi Watanabe*[1] , *Masato Kurihara*[2], *and Tohru Kawamoto*[1*]

[1] Nanomaterials Research Institute, National Institute of Advanced Industrial Science and Technology, 1-1-1 Higashi, Tsukuba, Ibaraki 305-8565, Japan.
[2] Department of Biological Chemistry, Faculty of Science, Yamagata University, 1-4-12 Kojirakawa-machi, Yamagata, Yamagata 990-8560, Japan
[*]E-mail: tohru.kawamoto@aist.go.jp; ORCID: orcid.org/0000-0002-3984-2980

Received: 9 December 2017 / *Accepted:* 16 February 2018 / *Published:* 10 April 2018

Multi-layered thin films exhibiting electrochromism have been developed using sequential coating processes with water-dispersible nanoparticles of metal (Fe, Ni) hexacyanoferrates. To fabricate the multi-layered films, a simple method is developed to avoid re-dispersion of the water-dispersible film using a dip-washing process in aqueous solutions of metallic salt. On the one hand, the thickness of the multi-coated film of the nanoparticles of iron hexacyanoferrate (FeHCF: Prussian blue) is estimated to be 100 nm, 190 nm, 300 nm, and 420 nm for single, double, triple, and quadruple layers, respectively, and the optical absorbance of the multi-coated film shows dense color proportional to the number of coatings. On the other hand, the double-layered film composed of FeHCF and nickel hexacyanoferrate (NiHCF) layers of thicknesses estimated to be 110 nm and 840 nm, respectively, shows electrochromism among green, blue, and colorless, where green is the blend of the colors of FeHCF and NiHCF.

Keywords: electrochromism, Prussian blue, metal hexacyanoferrate, nanoparticle, multilayered film, spin-coating

1. INTRODUCTION

Electrochromism (EC)[1–30], the color change of materials via electrochemical redox control, is expected to be applied to energy-conserving devices, e.g., low-energy-consuming reflective displays such as electronic papers, and color-switchable windows for improving air-conditioning efficiency of building or vehicles [4].

Among various EC materials, Prussian-blue-type complexes are fascinating because of their stable responses and variety of colors shown [1,2,31–49]. For example, Prussian blue (FeHCF,

$Fe[Fe(CN)_6]_x$) shows electrochromism in two steps [1]: the blue state ($Fe^{3+}[Fe^{II}(CN)_6]_x$) changes to colorless state ($Fe^{2+}[Fe^{II}(CN)_6]_x$) below the redox potential V_{red}=~ +0.2 V versus a saturated calomel electrode (vs. SCE), and to green or yellow state, including $Fe^{3+}[Fe^{III}(CN)_6]_x$ above V_{red} =~ +0.9 V (vs. SCE). Nickel-substituted analogue (NiHCF, $Ni[Fe(CN)_6]_y$) [32,48] exhibits a yellow state, $Ni^{2+}[Fe^{III}(CN)_6]_y$, and switches to the colorless state $Ni^{2+}[Fe^{II}(CN)_6]_y$ below V_{red} =~ +0.5 V (vs. SCE).

We have developed nanoparticles of various Prussian-blue-type complexes [37,49,50], using a simple, efficient, and low-cost procedure suitable for mass production; it provides dense "inks" of nanoparticles of > 0.1 g/mL, available for conventional coating liquid processes such as spin coating. In particular, water-dispersible nanoparticles provide additional advantages as they are environmentally friendly, inexpensive, and compatible with non-aqueous electrolyte solutions [31,38].

In this paper, we report a new method to fabricate multilayered EC films of the nanoparticles of Prussian-blue-type complexes in order to achieve various colors in electrochromism. The multilayered EC films are fabricated using sequential coating, prior to which each layer undergoes a non-elution process. A "non-eluting" film is defined as a film that is non-dispersible when dipped into water. Without the non-elution process, sequential coating is impossible because the layer of the water-dispersible nanoparticles dissolves in the water-based dispersion liquid of the subsequent coating process.

We have already reported that dipping a thin film into a solution of transition metal salts renders the water-dispersible copper-substituted FeHCF analogues film non-eluting [51]. In this paper, we reveal that this method is applicable to the fabrication of multi-layered thin films. Non-elution occurs with the decrease of polarity of the surface of nanoparticles owing to the coordination of the transition metal cations. The surface of the water-dispersible FeHCF (w-FeHCF) and the water-dispersible NiHCF (w-NiHCF) nanoparticles is negatively charged owing to their structure—core nanocrystals ($M[Fe(CN)_6]_x$, M=Fe, Ni) covered with hexacyanoferrate anions $[Fe(CN)_6]^{z-}$[49]. The polarity from the surface is negative, and helps the dispersion of the nanoparticle into polar solvents such as water. Adding cations into the nanoparticle ink would produce bondings with the hexacyanoferrate anions on the surface of nanoparticles, resulting in the cancellation of the surface charge of the nanoparticles. Cross-linking by the coordinating cations between hexacyanoferrate anions on the adjacent nanoparticles is also expected.

2. EXPERIMENTAL

The synthesis method of the w-FeHCF nanoparticles has already been reported in previous reports [31,49]. FeHCF nanocrystals, which are the core of the nanoparticles, were synthesized as the reaction product of (a) $Fe(NO_3)_3 \cdot 9H_2O$ and (b) $Na_4[Fe(CN)_6] \cdot 10H_2O$. The obtained precipitate was added into an aqueous solution of (c) $Na_4[Fe(CN)_6] \cdot 10H_2O$, where the molar ratio of reagents (a), (b), and (c) was 4:3:0.7. After stirring, a w-FeHCF nanoparticle ink was obtained.

The w-NiHCF nanoparticles were also obtained using a similar procedure. The yellow nanocrystalline precipitate of NiHCF obtained by mixing (d) $Ni(NO_3)_2 \cdot 9H_2O$ and (e) $K_3[Fe(CN)_6]$ was added into a solution of (f) $Na_4[Fe^{II}(CN)_6] \cdot 10H_2O$, where the molar ratio of reagents (d), (e), and (f)

was 3:2:0.5. A powder of the water-dispersible nanoparticles was obtained via vacuum evaporation to dryness.

The Prussian-blue-type crystal structure of the nanoparticles was confirmed using powder X-ray diffraction patterns. The mean number diameter of the nanoparticles, observed using dynamic light-scattering measurements (Nanotrac UPA-EX150; Microtrac Inc.), was 26.7 nm and 40.4 nm for w-FeHCF and w-NiHCF, respectively. The nanoparticle thin films were deposited on an indium tin oxide (ITO) substrate with a dispersion liquid of concentration 0.1 g/mL using the spin-coating method.

Before coating the second layer over the first nanoparticle thin film, the latter underwent non-elution in which the pre-fabricated film was quickly dipped into an aqueous solution of 0.1 mol/L $FeCl_3$ and rinsed with water for 20 s. It was also confirmed that aqueous solutions of several transition metals, e.g., $Fe(NO_3)_3$, $FeCl_2$, $NiCl_2$, and $Ni(NO_3)_2$, can be used for the non-elution of both w-FeHCF and w-NiHCF nanoparticles. Notably, the yellow w-NiHCF film dipped into $FeCl_2$ solution exhibited green color, which is the combination of the original yellow color of NiHCF and additional blue color of single FeHCF molecular layer caused by the coordinated iron cation and the hexacyanoferrate anion at the w-NiHCF surface [52].

Two films were prepared via non-elution: a thick film with sequential coatings of w-FeHCF nanoparticles ink, and a double-layered film with w-NiHCF and w-FeHCF nanoparticles ink. To investigate the films, a UV–Vis spectrometer (UV-USB4000; Ocean Optics Inc.) was used for optical measurement, a stylus-type surface profilometer (Alpha-step IQ; KLA Tencor Corp.) was used for thickness evaluation, and a field-emission scanning electron microscope (FE-SEM: S-4800, Hitachi High-Technologies) was used for cross-section analyses. A potentiostat (ALS-711B; BAS Inc.) was used for electrochemical investigations, with platinum wire as the counter electrode, SCE as the reference electrode, and 0.1M KPF_6/propylene carbonate solution as the electrolyte. All values of the potentials in this paper are indicated versus SCE.

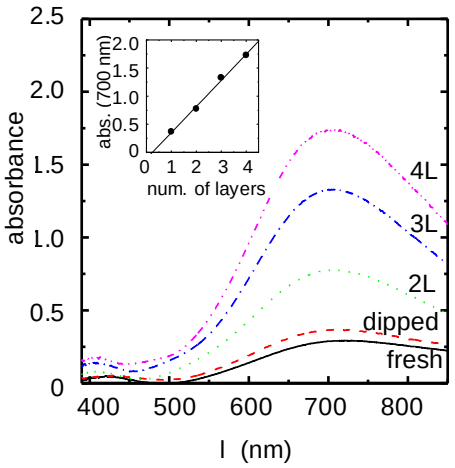

Figure 1. Optical absorbance spectra of the multilayered FeHCF nanoparticle films. "Fresh" and "dipped" represent the spin-coated w-FeHCF film without treatment and film poured with $FeCl_2$ aqueous solution, respectively. "2L," "3L," and "4L" represent the double-layered, triple-layered, and quadruple-layered films, respectively. Insets: Optical absorbance at λ= 700 nm of each layered film.

3. RESULTS AND DISCUSSION

The multilayered coating of the FeHCF nanoparticles in Fig. 1 shows optical absorbance proportional to the number of layers, and the measured film thickness is estimated to be 100 nm, 190 nm, 300 nm, and 420 nm for single, double, triple, and quadruple layers, respectively. These results indicate that each layer has almost the same thickness and exhibits the same optical properties. Note that the absorbance of the "non-eluted" film at 700 nm after dipping is slightly larger than that of the fresh film. This is also caused by the coordination of the iron cations onto the surface of nanoparticles. In the electrochemical measurement, the thick film obtained with quadruple coatings becomes colorless at −0.5 V, and returns to blue at +0.8 V, which is the same response as a single-coated film [31]. The quadruple-coated film shows color change even after 100 cycles of potential switch between −0.5 V for 30 s and +0.8 V for 30 s.

The NiHCF/FeHCF double-layered film is fabricated using sequential coatings of the w-NiHCF film on the w-FeHCF film. The double-layered structure can be observed in the cross-section analysis using FE-SEM as shown in Fig. 2. From this SEM image, the thickness of FeHCF and NiHCF layers is estimated to be 110 nm and 840 nm, respectively. The thickness of each layer is designed so that the multi-layered film shows green color, which is the mixture of blue color shown by w-FeHCF and yellow color shown by w-NiHCF. Figure 3(a) shows the optical absorbance of the single-layered FeHCF film and the NiHCF/FeHCF film. The NiHCF/FeHCF film shows two absorption bands at approximately λ= 400 nm and λ= 700 nm of the NiHCF/FeHCF film. These bands correspond to the absorption of FeHCF and NiHCF films, respectively. Figure 3(b) shows the cyclic voltammogram of the NiHCF/FeHCF film with three redox peaks corresponding to the redox reactions of FeHCF and NiHCF described in Sec. 1. This result demonstrates that the redox reaction of each film can occur separately, i.e., the three reduction waves appearing around +0.1 V, +0.5 V, and +0.8 V correspond to the reduction of Fe^{3+} in FeHCF, $[Fe(CN)_6]^{3-}$ in NiHCF, and $[Fe(CN)_6]^{3-}$ in FeHCF, respectively. The first oxidation wave corresponds to the oxidation of Fe^{2+} in FeHCF and the second oxidation wave with a shoulder is caused by the overlapping of the oxidation of $[Fe(CN)_6]^{4-}$ in NiHCF and $[Fe(CN)_6]^{4-}$ in FeHCF. These assignments are supported by the optical measurement under a step-like potential change shown later.

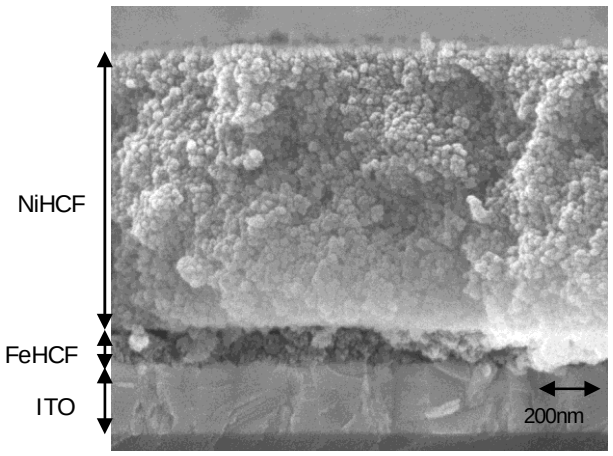

Figure 2. FE-SEM image of the cross-section of a NiHCF/FeHCF/ITO film

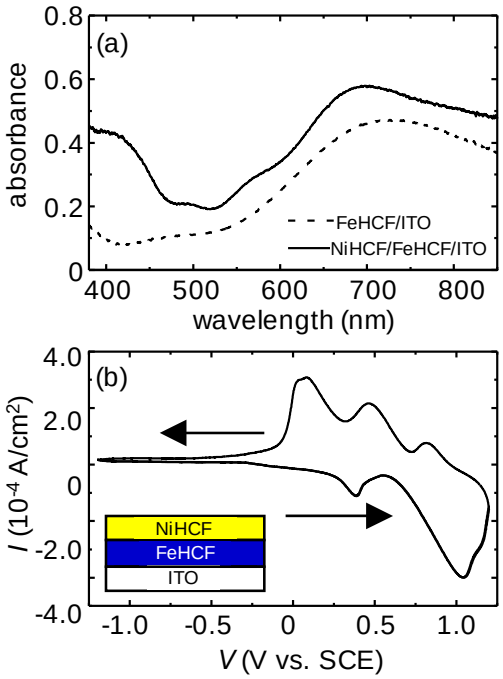

Figure 3. (a) Optical absorbance of the FeHCF/ITO film and NiHCF/FeHCF/ITO film. (b) Cyclic voltammogram of the NiHCF/FeHCF/ITO film obtained as the second cycle in the sequential cycling at the scan rate of 5 mV/s.

We observed that the NiHCF/FeHCF film exhibits electrochromism between colorless and green, which the mixture of blue color shown by w-FeHCF and yellow color shown by w-NiHCF. Figure 4 shows the transmittance T(λ) at the wavelengths λ= 400 nm and 700 nm of the w-NiHCF/w-FeHCF film by applying potential with step-like changes. In the segments with V= −1.0 V (vs. SCE), both T(400 nm) and T(700 nm) are approximately 80%, indicating that both FeHCF and NiHCF are in colorless states. In the case of V > +0.5 V (vs. SCE), T(700 nm) decreases by approximately 40–50% corresponding the oxidation of w-FeHCF into blue state, because the redox potential of w-FeHCF is approximately +0.2 V (vs. SCE). However, the behavior of T(400 nm) is different, because the redox potential of w-NiHCF is approximately +0.5 V (vs. SCE). When V= +0.5 V (vs. SCE), T(400 nm) changes very slowly and remains a rather large value, and the film color is blue. At V= +0.7 V (vs. SCE), T(400 nm) becomes a lower value, and the film becomes green, which is the superimposed color of blue FeHCF and yellow NiHCF. Finally, in the case of V= +0.9 V, T(400 nm) shows the lowest value and T(700 nm) slightly rises, indicating that FeHCF is partially converted to $Fe^{3+}[Fe^{III}(CN)_6]_x$. Thus, the redox reaction of the NiHCF/FeHCF film can be understood as the combination of the individual films.

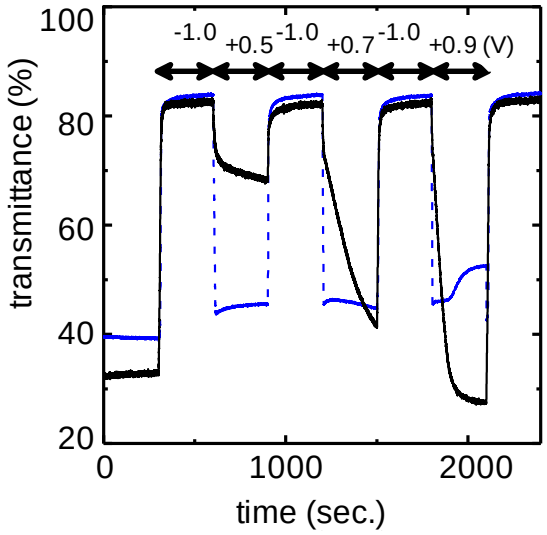

Figure 4. Optical transmittance T(λ) at the wavelengths λ= 400 nm (black line) and 700 nm (blue line) of the NiHCF/FeHCF/ITO film during step-like change of potential V.

Finally, our films and their electrochromic performance are compared with the results of the previous studies. A few studies fabricated multi-layered films with metal hexacyanoferrate (MHCF). [21,22,24,46,53]. The multi-layered films in these reports were prepared via two kinds of fabrication methods. One is the layer-by-layer method with alternate deposition of layers of MHCF nanoparticles and other materials. The other is the synthesis of MHCF on a substrate via the sequential dipping of metal cations and hexacyanoferrate anion. The advantage of our approach in comparison with these methods is that a pure MHCF film can be prepared with fewer processes without using other materials. Both previous methods require repeated processes for the preparation of a thicker film for denser coloration. In contrast, as shown in Fig. 2, film with a large thickness of ~1 μm can be easily fabricated using our method.

In addition, our method would be helpful for other application of MHCF films such as battery electrodes [54,55], sensors [56,57], and adsorbents for gaseous molecules [58] and ions [59].

4. CONCLUSION

The multilayered films of water-dispersible nanoparticles of metal hexacyanoferrates fabricated using sequential coatings exhibited electrochromism, which can be understood as the combination of the individual films. An effective new method involving dipping the film into a solution of metallic salts was used to prepare the multilayered films. As nanoparticles of various FeHCF analogues have been developed [30,60,61], this method is promising for the fabrication of multilayered films exhibiting electrochromism with various colors.

ACKNOWLEDGEMENTS
The authors acknowledge Drs. N. Minami and S. Kazaoui for their support with dynamic light-scattering measurements and Mr. T. Kiyoshi for his support with FE-SEM measurements.

References

1. V. D. Neff, *J. Electrochem. Soc.*, 125 (1978) 886.
2. K. Itaya, T. Ataka and S. Toshima, *J. Am. Chem. Soc.*, 104 (1982) 4767.
3. N. L. Sbar, L. Podbelski, H. Yang and B. Pease, *Int. J. Sustain. Built Environ.*, 1 (2012) 125.
4. J. Barratt and K. Dowd, *Des. Manag. Rev.*, 17 (2010) 25.
5. K. Itaya, K. Shibayama, H. Akahoshi and S. Toshima, *J. Appl. Phys.*, 53 (1982) 804.
6. T. Kobayashi, H. Yoneyama and H. Tamura, *J. Electroanal. Chem. Interfacial Electrochem.*, 161 (1984) 419.
7. P. M. Beaujuge and J. R. Reynolds, *Chem. Rev.*, 110 (2010) 268.
8. C. G. Granqvist, *Sol. Energy Mater. Sol. Cells*, 60 (2000) 201.
9. S. K. Deb, *Sol. Energy Mater. Sol. Cells*, 92 (2008) 245.
10. R. J. Mortimer, *Electrochim. Acta*, 44 (1999) 2971.
11. C. M. Lampert, *Sol. Energy Mater.*, 11 (1984) 1.
12. D. R. Rosseinsky and R. J. Mortimer, *Adv. Mater.*, 13 (2001) 783.
13. G. A. Niklasson and C. G. Granqvist, *J. Mater. Chem.*, 17 (2007) 127.
14. R. J. Mortimer, *Chem. Soc. Rev.*, 26 (1997) 147.
15. C. Hsu, J. Zhang, T. Sato, S. Moriyama and M. Higuchi, *ACS Appl. Mater. Interfaces*, 7 (2015) 18266.
16. F. Han, M. Higuchi and D. G. Kurth, *Adv. Mater.*, 19 (2007) 3928.
17. S. Araki, K. Nakamura, K. Kobayashi, A. Tsuboi and N. Kobayashi, *Adv. Mater.*, 24 (2012) OP122.
18. K. Tajima, Y. Yamada, M. Okada and K. Yoshimura, *Sol. Energy Mater. Sol. Cells*, 94 (2010) 1716.
19. K. Tajima, Y. Yamada, M. Okada and K. Yoshimura, *Appl. Phys. Express*, 3 (2010) 42201.
20. B. Kong, C. Selomulya, G. Zheng, D. Zhao, G. Kettlgruber, I. Graz, S. Aazou, C. Ulbricht, D.A. Egbe, M. C. Miron, H. Sun, B. Frisch and F. Boulmedais, *Chem. Soc. Rev.*, 44 (2015) 7997.
21. S. Al Shaal, F. Karabet and H. Kellawi, *Indian J. Chem.*, 56A (2017) 767.
22. S. Bharathi, M. Nogami and S. Ikeda, *Langmuir*, 17 (2001) 7468.
23. C. Hu, T. Kawamoto, H. Tanaka, A. Takahashi, K. Lee, S. Kao, Y. Liao and K. Ho, *J. Mater. Chem. C*, 4 (2016) 10293.
24. X. Liu, A. Zhou, Y. Dou, T. Pan, M. Shao, J. Han and M. Wei, *Nanoscale*, 7 (2015) 17088.
25. G. N. Calaça, C. A. Erdmann, A. L. Soares, C. A. Pessôa, S. T. Fujiwara, J. R. Garcia, M. Vidotti and K. Wohnrath, *Electrochim. Acta*, 249 (2017) 104.
26. J. Qian, D. Ma, Z. Xu, D. Li and J. Wang, *Sol. Energy Mater. Sol. Cells*, (2017).
27. H. Liao, T. Liao, W. Chen, C. Chang and L. Chen, *Sol. Energy Mater. Sol. Cells*, 145 (2016) 8.
28. H. Lu, S. Kao, T. Chang, C. Kung and K. Ho, *Sol. Energy Mater. Sol. Cells*, 147 (2016) 75.
29. M. Fan, S. Kao, T. Chang, R. Vittal and K. Ho, *Sol. Energy Mater. Sol. Cells*, 145 (2016) 35.
30. T. Liao, W. Chen, H. Liao and L. Chen, *Sol. Energy Mater. Sol. Cells*, 145 (2016) 26.
31. H. Shiozaki, T. Kawamoto, H. Tanaka, S. Hara, M. Tokumoto, A. Gotoh, T. Satoh, M. Ishizaki, M. Kurihara and M. Sakamoto, *Jpn. J. Appl. Phys.*, 47 (2008) 1242.
32. S. Hara, H. Tanaka, T. Kawamoto, M. Tokumoto, M. Yamada, A. Gotoh, H. Uchida, M. Kurihara and M. Sakamoto, *Jpn. J. Appl. Phys.*, 46 (2007) L945.
33. K. Ho, T. G. Rukavina and C.B. Greenberg, *J. Electrochem. Soc.*, 141 (1994) 2061.
34. K. Chen, C. Hsu, C. Hu and K. Ho, *Sol. Energy Mater. Sol. Cells*, 95 (2011) 2238.
35. A. Kraft and M. Rottmann, *Sol. Energy Mater. Sol. Cells*, 93 (2009) 2088.
36. D. M. DeLongchamp and P. T. Hammond, *Adv. Funct. Mater.*, 14 (2004) 224.
37. M. Ishizaki, K. Kanaizuka, M. Abe, Y. Hoshi, M. Sakamoto, T. Kawamoto, H. Tanaka and M. Kurihara, *Green Chem.*, 14 (2012) 1537.

38. K. Lee, H. Tanaka, A. Takahashi, K.H. Kim, M. Kawamura, Y. Abe and T. Kawamoto, *Electrochim. Acta*, 163 (2015) 288.
39. E. Nossol and A. J. G. Zarbin, *Sol. Energy Mater. Sol. Cells*, 109 (2013) 40.
40. S. Itaya, Klngo; Shibayama, Kimio; Akahoshi, Haruo; Toshima, *J. Appl. Phys.*, 53 (1982) 804.
41. L. M. N. Assis, J. R. Andrade, L. H. E. Santos, A. J. Motheo, B. Hajduk, M. Łapkowski and A. Pawlicka, *Electrochim. Acta*, 175 (2015) 176.
42. S. Pahal, M. Deepa, S. Bhandari, K. Sood and A. Srivastava, *Sol. Energy Mater. Sol. Cells*, 94 (2010) 1064.
43. M. Berrettoni, M. Giorgetti, S. Zamponi, P. Conti, D. Ranganathan, A. Zanotto, M. Saladino and E. Caponetti, *J. Phys. Chem. C*, 114 (2010) 6401.
44. S. Hong and L. Chen, *Electrochim. Acta*, 55 (2010) 3966.
45. A. Zloczewska, A. Celebanska, K. Szot, D. Tomaszewska, M. Opallo and M. Jönsson-Niedziolka, *Biosens. Bioelectron.*, 54 (2014) 455.
46. C. Shan, L. Wang, D. Han, F. Li, Q. Zhang, X. Zhang and L. Niu, *Thin Solid Films*, 534 (2013) 572.
47. J. Wang, X. Sun and Z. Jiao, *Materials (Basel).*, 3 (2010) 5029.
48. O. Sato, *J. Solid State Electrochem.*, 11 (2007) 773.
49. A. Gotoh, H. Uchida, M. Ishizaki, T. Satoh, S. Kaga, S. Okamoto, M. Ohta, M. Sakamoto, T. Kawamoto, H. Tanaka, M. Tokumoto, S. Hara, H. Shiozaki, M. Yamada, M. Miyake and M. Kurihara, *Nanotechnology*, 18 (2007) 345609.
50. K. Ono, M. Ishizaki, S. Soma, K. Kanaizuka, T. Togashi and M. Kurihara, *RSC Adv.*, 5 (2015) 96297.
51. K. Lee, A. Takahashi, H. Tanaka, K.H. Kim, M. Kawamura, Y. Abe, M. Ishizaki, M. Kurihara and T. Kawamoto, *Bull. Chem. Soc. Jpn.*, 88 (2015) 1561.
52. M. Ishizaki, Y. Sajima, S. Tsuruta, A. Gotoh, M. Sakamoto, T. Kawamoto, H. Tanaka and M. Kurihara, *Chem. Lett.*, 38 (2009) 1058.
53. D. M. DeLongchamp, M. Kastantin and P. T. Hammond, *Chem. Mater.*, 15 (2003) 1575.
54. P. Nie, L. Shen, H. Luo, B. Ding, G. Xu, J. Wang and X. Zhang, *J. Mater. Chem. A*, 2 (2014) 5852.
55. Y. Moritomo, K. Goto and T. Shibata, *Energies*, 8 (2015) 9486.
56. X. Zhai, Y. Li, J. Li, C. Yue and X. Lei, *Mater. Sci. Eng. C*, 77 (2017) 1242.
57. J. Zhao, P. Yue, S. Tricard, T. Pang, Y. Yang and J. Fang, *Sensors Actuators B Chem.*, 251 (2017) 706.
58. A. Takahashi, H. Tanaka, D. Parajuli, T. Nakamura, K. Minami, Y. Sugiyama, Y. Hakuta, S. Ohkoshi and T. Kawamoto, *J. Am. Chem. Soc.*, 138 (2016) 6376.
59. R. Chen, H. Tanaka, T. Kawamoto, M. Asai, C. Fukushima, H. Na, M. Kurihara, M. Watanabe, M. Arisaka and T. Nankawa, *Electrochim. Acta*, 87 (2013) 119.
60. M. Ishizaki, A. Gotoh, M. Abe, M. Sakamoto, H. Tanaka, T. Kawamoto and M. Kurihara, *Chem. Lett.*, 39 (2010) 762.
61. M. Ishizaki, M. Sakamoto, H. Tanaka, T. Kawamoto and M. Kurihara, *Mol. Cryst. Liq. Cryst.*, 539 (2011) 18/[358].